Intermetallics 71 (2016) 12–17

Contents lists available at ScienceDirect

Intermetallics

journal homepage: www.elsevier.com/locate/intermet

An index of shear banding susceptibility of metallic glasses

M. Zhang, Y. Chen, L.H. Dai*

State Key Laboratory of Nonlinear Mechanics, Institute of Mechanics, Chinese Academy of Sciences, Beijing 100190, China

ARTICLE INFO

Article history:
Received 29 September 2015
Received in revised form
10 November 2015
Accepted 26 November 2015
Available online xxx

Keywords:
Metallic glasses
Inhomogeneous deformation
Shear band
Mechanical properties
Theory

ABSTRACT

By virtue of instability analysis, an index of shear banding susceptibility of metallic glasses (MGs): the critical strain localization factor to initiate an embryonic shear band:$\chi = \gamma_b/\gamma_m$ (γ_b shear strain in the embryonic shear band and γ_m in the matrix) is derived in analogue to the emergence of geometrically necessary dislocations (GND) in crystals. Physical properties, like Poisson ratioυ, Young's modulus E and the surface energy density ζ, are explicitly incorporated into the formulae of χ with which the origin of the plasticity of MGs are unraveled.

1. Introduction

The plasticity of metallic glasses (MGs) [1–3] mainly consists of local non-affine atomic rearrangements which are highly susceptible to extremely localized shear banding [4–8]. Notoriously, the susceptibility to shear banding in MGs [9–11] is challenging for the limited temporal/spatial scale of shear banding (of 10–20 nm in thickness and operating at a strain rate of 10^4–10^5 s^{-1}) [12] and outrageous tension-compression asymmetry [13,14]. Even the Zr-riched MGs which can achieve extended compressive plasticity (>50%) [15] mediated by multiplied shear bands, reveal disastrous fracture via a single shear band under uniaxial tension. Also true is that the Pd-riched MG [16] with superior toughness (~200 MPa $m^{1/2}$) for significant shear band proliferation also exhibits similar tensile single-shear banding failure. The prevailing picture [4,17] of shear banding in MGs is depicted in Fig. 1. A shear localized zone propagates from a random stress concentrator at sound speed level to form an embryonic shear band, and then it develops into an unstable mature shear band with a clear slip offset. The essential character of shear band is the localized shear strain inside. Hence, the critical strain localization intensity in the embryonic shear band is the key to the susceptibility of shear banding and the diverse plasticity of MGs.

2. Shear banding susceptibility

As having been used in previous works [1,18], the critical strain localization factor to initiate an embryonic shear band:$\chi = \gamma_b/\gamma_m$ (γ_b shear strain in the embryonic shear band and γ_m in the matrix) is a natural index to study the susceptibility of shear banding in metallic glasses. However, to evaluate this shear localization factor is nontrivial, because that the unstable nature of a mature shear band under unaxial load hinders a thorough investigation on shear banding and that extrinsic factors like the stiffness of the test machine also [19] steps in. Whereas, in bend the propagation of shear bands is largely suppressed by the stress gradient [16,20], leaving an access out of the straits by assuming that the critical strain localization factor is an intrinsic property of MGs (i.e., not depending on the load conditions).

Fig. 2 shows the bended morphology of (Vit1) $Zr_{41.2}Ti_{13.8}Cu_{10}Ni_{12.5}Be_{22.5}$ MG where shear bands in periodical distribution [21–23] emerges. Intuitively, the stress gradient and the periodicity of shear bands suggest a meniscus instability-related shear band incubation behavior, because that the meniscus instability originating from periodical perturbations is also provoked by a stress gradient. The development of the perturbation would induce stress concentrators (in Fig. 1) required for the initiation of an embryonic shear band. More generally, to accommodate the strain gradients and minimize the strain energy in bended crystalline materials due to the inhomogeneous deformation at atomic scale (e.g. dislocation interaction, twinning and grain boundary gliding), a periodical distribution of geometrically necessary dislocations (GND) [24–26]

* Corresponding author.
E-mail address: lhdai@lnm.imech.ac.cn (L.H. Dai).

http://dx.doi.org/10.1016/j.intermet.2015.11.010

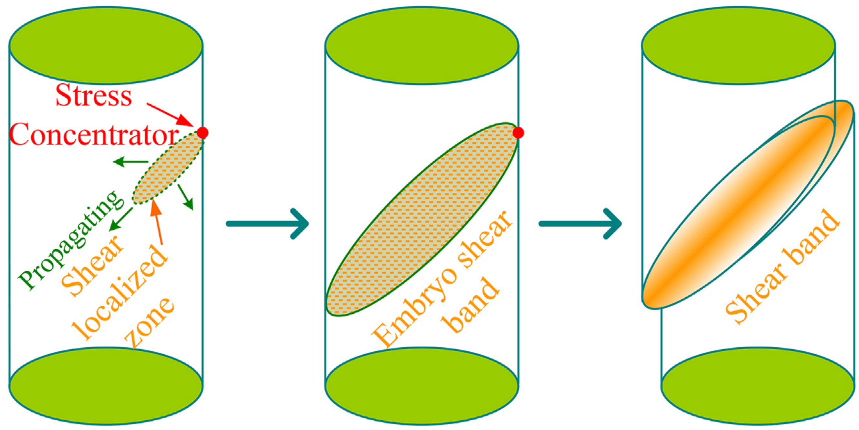

Fig. 1. Schematic illustration of shear banding in metallic glasses.

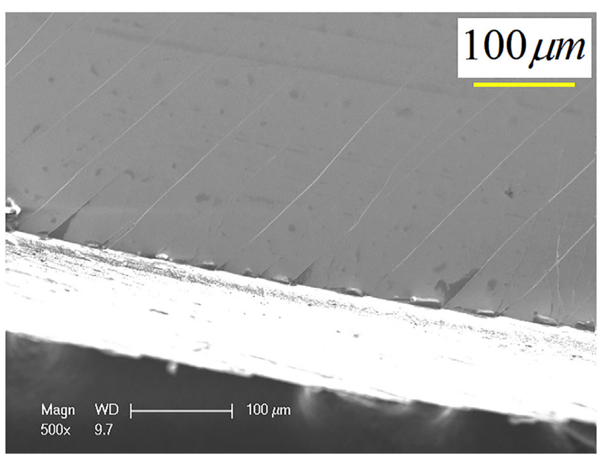

Fig. 2. Periodically distributed shear bands on the side surface of Vit1 metallic glass.

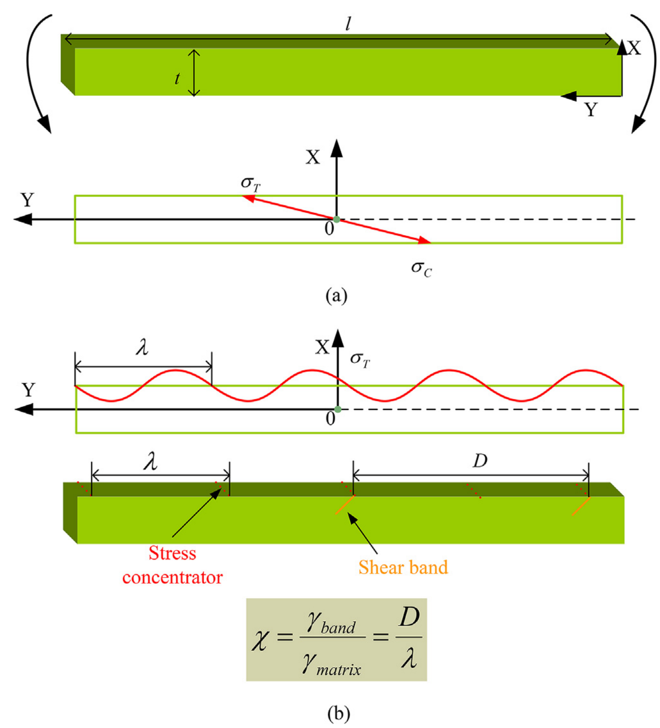

Fig. 3. Instability analysis on the precipitation of periodically distributed shear bands in the bend of metallic glasses. (a) Illustration of the bend deformation and the stress distribution along the cross section of the beam, where the plane strain condition is assumed; (b) the critical wavelength λ and the shear band space *D*.

emerges. Via coarse graining, at a characteristic mesoscopic length scale which is several dozens of times (approximately 10–100) of the space between the GNDs, the distortion of the lattice vanishes for the periodic distribution of the GNDs which corresponds to the minimum strain energy configuration [27]. It has been known that shear bands in MGs plays the equivalent role to dislocations in crystals during plastic deformation. Also for the inhomogeneous atomic scale deformation mechanism in MGs (e.g. local atomic rearrangement confined by its surrounding elastic matrix and shear bands), the periodicity of the shear bands in Fig. 2 would imply similar emerging dynamics to GNDs from the shear banding incubation sites for strain energy minimization as constrained by the geometric compatibility conditions. In this work, by considering the incubation and the emergence of shear bands in bend separately, we manage to provide a solution to the index of shear banding susceptibility $\chi = \gamma_b/\gamma_m$ of MGs.

3. Application

Suppose a beam in bend of a length of *l* and a thickness of *t* as shown in Fig. 3(a). The plane strain condition is assumed, i.e. an infinite width in the direction normal to *XY* plane. With increasing external load, the stress on the upper and bottom surfaces of the beam would reach the yielding strength σ_y firstly. We would like to consider the very instant that the upper or the bottom surface yields ($\sigma = \sigma_y$). The localized shear banding can be considered as a result of the perturbation triggered instability in homogeneous deformation [1]. According to the displacement boundary conditions, the perturbation here is prescribed as a periodical fluctuation on the surface of the beam. By virtue of routine instability analysis as presented in the next section, it is easy to find that the crests of an infinitesimal perturbation with a critical wavelength λ will develop into sustaining stress concentrators. Recalling the stress concentrator where shear localized zone initiates, the perturbation are potential shear band incubation sites to trigger shear bands as illustrated in Fig. 3(b).

The instability analysis is conducted as follows. For the absence of work-hardening mechanisms in MGs, it is taken as an ideal plastic solid. As shown in Fig. 4, assuming the upper surface of the beam with a perturbation δe of periodic λ is under compression in

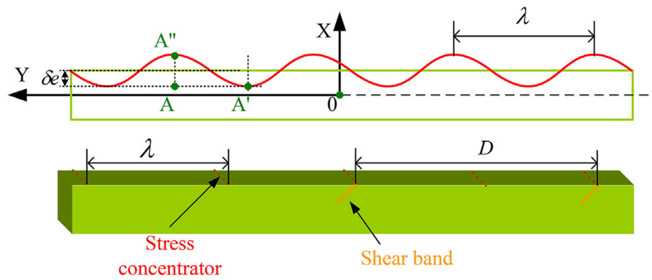

Fig. 4. Illustration of the instability analysis.

bend, the stresses at the crest A′ is $\sigma_{A'} = \sigma_y - \zeta 2\pi(2\pi/\lambda)^2\delta e$ for the surface tension caused by the increasing curvature. The stress at point A is $\sigma_A = \sigma_y - d\sigma/dx\delta e$. The stress at the troughs A″ is σ_y, for the ideal plastic assumption. This is exactly the same scenario to the meniscus instability analysis conducted by Argon and Salama [28]. The crests of the perturbation of specific wavelength λ would develop into sustaining periodical stress concentrators along the yielded beam surface, provided that the stresses at point A and A′ satisfy:

$$\sigma_A = \sigma_y - \frac{d\sigma}{dx}\delta e \le \sigma_{A'} = \sigma_y - \zeta\left(\frac{2\pi}{\lambda}\right)^2\delta e. \quad (1)$$

Similar analysis can be conducted on the tensile side of the beam along the same route of analysis and consistent results can be obtained. Assuming the upper surface of the beam with a perturbation of periodic λ is under tension in bend. On the crests of the perturbation at A′, the stress is the yield strength σ_y. On the troughs of the perturbation A″, the stress is $\sigma_{A''} = \sigma_y - \zeta(2\pi/\lambda)^2\delta e$, for the surface tension caused by the increasing curvature. At point A, the stress is $\sigma_A = \sigma_y - \frac{d\sigma}{dx}\delta e$. For the stress gradient on the tensile side of the beam in bend, as long as the stress at point A″ exceeds the stress at A, the troughs of the perturbation would be a stable configuration, or else it would disappear. Thus, in analogue to meniscus instability analysis [28], the crests of the perturbation of specific wavelength λ would develop into sustaining periodical stress concentrators along the yielded beam surface, provided that:

$$\sigma_A = \sigma_y - \frac{d\sigma}{dx}\delta e \le \sigma_{A''} = \sigma_y - \zeta\left(\frac{2\pi}{\lambda}\right)^2\delta e \quad (2)$$

The expression is of exactly the same form to that of the case of compression and indicates the unified shear bands incubation behavior on both the tensile side and the compressive side in bend. Consequently, in consistent with the meniscus instability analysis, the criterion also reads [28]:

$$\frac{d\sigma}{dx} \ge \zeta\left(\frac{2\pi}{\lambda}\right)^2 \quad (3)$$

where ζ is the surface energy density (i.e. the surface tension). The stress gradient in bend reads: $d\sigma/dx = E/1 - \upsilon^2 \cdot 1/R = \alpha E/1 - \upsilon^2$, with $\alpha = 1/R \approx 1/25t$ by assuming the elastic limit of MGs is 2% [29], where E is the Young's modulus, υ is Poisson ratio, R is bend radius. Therefore, $\lambda \ge 2\pi\sqrt{\zeta(1-\upsilon^2)/\alpha E}$ gives the minimum space between two adjacent potential shear band incubation sites on the beam surface. This expression corroborates well the fact that tough MGs exhibit more shear bands, because a minimum incubation site space determines the superior limit of shear band multiplication and energy dissipation [16]. In analogue to the distribution of GNDs in crystals to minimize the strain energy, noting the geometric compatibility constrains on shear banding, to concentrate enough shear strain in an embryonic shear band, as shown in Fig. 3(b), the shear band space D should surpass the incubation site space λ by a factor $\chi = \gamma_b/\gamma_m$ (γ_b shear strain in the embryonic shear band and γ_m in the matrix) of which the value is also approximated to be 1–100 [17,30,31]. As the nature of shear banding is shear localization, the factor $\chi = \gamma_b/\gamma_m$ characterizing the critical shear localization intensity to initiate an embryonic shear band indicates the susceptibility of shear banding in MGs. Smaller χ stands for higher shear banding susceptibility and more significant shear band multiplication and better plasticity, and *vice versa*. Finally, the shear banding susceptibility of MGs can be written as:

$$\chi = \frac{D}{\lambda} = D \Bigg/ 2\pi\sqrt{\frac{\zeta(1-\upsilon^2)}{\alpha E}} \quad (4)$$

The generalization of Eq. (4) to uniaxial loading can be explained as follows. It is noted that our work is considering only the yielding point and the incipient shear banding plasticity of metallic glasses and that as shown in Fig. 1, shear bands nucleate from stress concentrators. The formation of completely different shear band morphologies in bend and in unaxial loading (compression and tension) which closely depend on the evolution dynamics of the embryonic shear bands would be another important problem worth more sophisticated investigation. Bearing these two points in mind, the scenarios of bend and unixial loading can be unified by a mathematically rigorous extrapolation. Based on the instability analysis above, by extrapolating the bend curvature $\alpha = 1/R \approx 1/25t$ of the yielded beam surface to 0, i.e., $t \to +\infty$, considering a beam of infinite thickness, in this limiting case, the stress gradient along y axis $d\sigma/dx = \alpha E/1 - \upsilon^2 = 0$ and the stress state of the beam surface is exactly in uniaxial tension or compression. As indicated by Eq. (3), with a stress gradient $d\sigma/dx = 0$ under unaxial loading condition, the critical wavelength of the instable perturbation $\lambda \ge 2\pi\sqrt{\chi \cdot (d\sigma/dx)^{-1}}$ would be infinite. Hence, an infinite shear band space D under uniaxial load is predicted. This matches the fact that most MGs would prefer fracturing via a single shear band under uniaxial load, especially under tension. More discussion on this issue will be presented in next section.

4. Results and discussion

The shear band space D in the bend of MGs has been readily examined in experimental tests [22,23]. Table 1 shows the shear banding susceptibility of several typical MG systems which exhibits different compression plasticity based on the measured shear band space in the bend tests both conducted previously and in this work as well. The detailed experimental procedure can be found in the Supplementary Materials. It can be seen that the calculated χ lying in the range (1–100) matches the simulation results [17,30] and well correlates with the compressive plasticity ε and fracture toughness K_Q of the MGs. This range of χ also coincides with that of the ratio of the characteristic length scale at which the lattice distortion vanishes to the average GNDs space [32]. This result suggests a universal geometric compatibility effect in the plastic deformation of solids. It is important to note the fact that the plastic deformation mechanisms of MGs are quite different from those of crystals. For the lack of work-hardening mechanism in MGs, the localized shear strain afforded by the activation of atomic level shear transformation zones (STZ) would accumulate in the stress concentrator. With enough number of STZs activated and sufficient shear strain localized, i.e., the critical shear localization ratio (the shear banding susceptibility index) is reached, embryonic shear

Table 1
Shear banding susceptibility of several metallic glasses.

Metallic glasses	K_Q(MPa m$^{1/2}$)[a]	D(μm)	ε(%)	ζ(J/m^2)[b]	υ[b]	E(GPa)[c]	λ(μm)	χ	Ref.
$Zr_{64.13}Cu_{15.75}Ni_{10.12}Al_{10}$	~86 [33]	55	>50 [15]	~2	0.38	78.4	4.64	11.8	[34]
$Cu_{47.5}Zr_{47.5}Al_5$	~100 [35]	55	10.9 [36]	~2	0.37	89	4.37	12.6	–
$Pd_{79}Ag_{3.5}P_6Si_{9.5}Ge_2$	200	45	–	~2	0.42	88	4.29	10.49	[16]
$Pt_{74.7}Ag_{0.3}P_{18}B_4Si_{1.5}Cu_{1.5}$	125	45	>40	~2.5	0.43	92.7	4.67	9.63	[20]
$Pt_{57.5}Cu_{14.7}Ni_{5.3}P_{22.5}$	80	45	20	~2.5	0.42	94.8	4.63	9.72	[37]
$Zr_{57}Nb_5Al_{10}Cu_{15.4}Ni_{12.6}$	32.7 [38]	~95	0.5 [39]	~2	0.36	87.3	4.43	21.5	[22]
$Pd_{40}Cu_{30}Ni_{10}P_{20}$	–	~150	0 [40]	~2	0.40	99.8	4.07	~36.8	–
$La_{62}Al_{14}Ag_{2.34}Ni_{10.83}Co_{10.83}$	~5 [41]	~180	0 [42]	~1	0.35	33	5.12	~35.2	–
$Zr_{41.2}Ti_{13.8}Cu_{10}Ni_{12.5}Be_{22.5}$(Vit1)	55 [43]	~75	1.5 [36]	~2	0.35	94.3	4.28	17.5	–

[a] Some MGs are estimated as the value of similar composition.
[b] The data are estimated as the value of the main constituent element Ref. [44].
[c] Ref. [45].

bands would emerge as illustrated in Figs. 3 and 4. In a different case, for the work-hardening mechanisms of crystals due to the interaction between crystal defects (like dislocations, grain boundaries and so on), the work-hardening effect would prevent the deformation of the stress concentrators from continuous strain localization. Therefore, accompanying further loading, the crystal beam would deformation homogeneously rather than like the MGs develop into shear banding.

On the other hand, many continuum scale modeling works focusing on the shear band space D in bend via momentum diffusion and energy dissipation have been conducted [22,23]. By introducing previous results [23] into Eq. (4), we can arrive at the analytical expression for the shear banding susceptibility χ:

$$\chi = \frac{D}{\lambda} = \sqrt{\frac{6\sigma_0 \beta \Lambda k (t - t_0)}{\rho(1 - \beta\Lambda/2)\omega\dot{\gamma}^2 \sin^2\theta}} \Bigg/ 2\pi\sqrt{\frac{\zeta(1 - \upsilon^2)}{\alpha E}} \quad (5)$$

The expression D is from Ref. [23]. The parameters are referred to the original work [23], where σ_0 is the yield strength; ρ is density; θ is the shear band angle; $\dot{\gamma}$ is strain rate inside the shear band; $\beta\Lambda$ is the shear dilatation coefficient; ω is the pressure-dependence coefficient; k is bending curvature; t_0 is the thickness of the elastic region. It can be seen that the thickness dependence of the shear band space satisfy: $D \propto (t - t_0)^{1/2}$. Similar expression can also be established based on other works [22]. However, the strain rate inside the shear band $\dot{\gamma}$, the shear dilatation coefficient $\beta\Lambda$ and the pressure-dependence coefficient ω are mainly estimated empirically and limits the application of Eq. (5). This is another reason that we focus on the shear band initiation in here. The initiation of embryonic shear bands is intrinsic to the plasticity of metallic glasses. As the denominator essentially determines the incipient shear band incubation, the numerator D mainly originates from the propagation of the embryonic shear bands. Therefore, one could alternatively define $\kappa = 1/\chi$ as the instability index of the shear band propagation process, with $\kappa = 1$ standing for steady homogeneous deformation, whereas the more κ approaching 0, the more dangerous the situation.

Since we would like to focus on the susceptibility of shear banding, the physics of the denominator λ in Eq. (4) which incorporates the intrinsic properties, such as Poisson ratio υ, Young's modulus E and the surface energy density ζ attracts us over the shear band space D. Fig. 5 shows the graphical presentation of λ. It can be seen that the MGs with high Young's modulus E, Poisson ratio υ would show small λ, i.e., high shear banding susceptibility. This is in good consistence with the reported damage tolerant MG [16] and the ductile PtCu-riched MG [37], which exhibit an E~90 GPa and a Poisson ratio υ~0.42. It is interesting to note that the υ dependence of λ is $\lambda \propto \sqrt{1 - \upsilon^2}$. This means that the dependence of shear band proliferation and plasticity of MGs on υ is reasonably

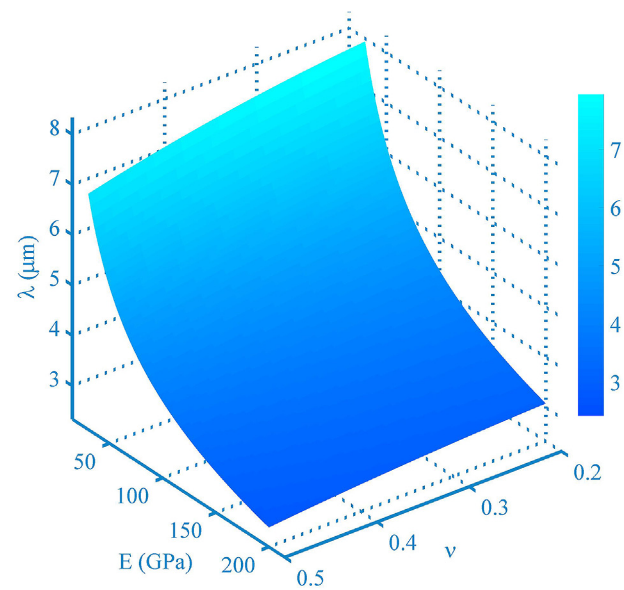

Fig. 5. Dependence of the critical wavelength λ from Eq. (3) on Poisson ratio υ and Young's modulus E, where $\zeta = 2$ (J/m^2) is adopted.

weak for the small value of $\upsilon \sim (0.2 - 0.5)$. It would rationalize why the Pd-riched MGs with similar $\upsilon = 0.40$ but exhibit rather poor ductility [46]. It is also important to note that the surface energy density ζ accounts for the chemical effect and the composition dependence of the shear band susceptibility plays a crucial role: $\lambda \propto \sqrt{\zeta}$. This explains why the FeCrMo-riched MGs [45] with appreciable E(200 GPa) but high ζ(3 J/m^2) and poor υ (0.3) show less shear banding susceptibility and poor ductility. The thickness dependence of shear band space D in bend is also predicted by Eq. (4), as smaller t induces smaller D. It is also noted that the derived dependence of D on sample thickness $D \propto t^{\frac{1}{2}}$ is also consistent with previous works as shown in Fig. 6.

Generally, Eq. (4) demonstrates the role of stress gradients in the incubation of shear bands in MGs, because that the initiation of shear banding is always attributed to the stress concentrators of MGs, namely, local defects or the sites where free volume accumulates [1], where both scenarios associate with stress gradients. Stress gradients enhanced shear banding propensity of MGs have widely been proved, such as indentation where severe stress gradients beneath the indenter trigger large amounts of shear bands [47], the stress gradients introduced by shot peening [48] or drawing [49] leading to pronounced shear bands proliferation and the stress gradients introduced via adjusting the shape of MGs, like the aspect ratio [50,51], the notch [52] and the unparalleled ends

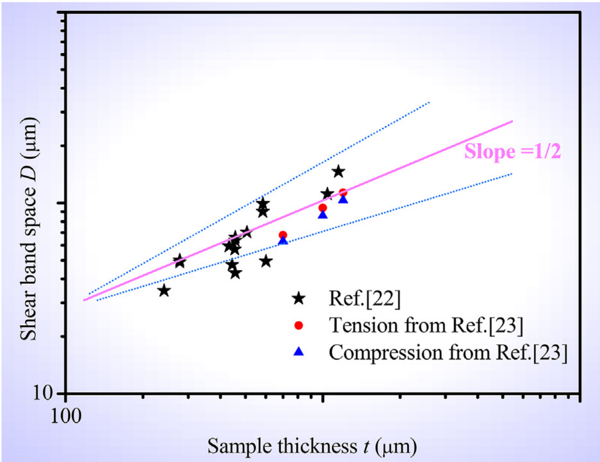

Fig. 6. The thickness t dependent shear band space D of metallic glasses.

[53]. Looking into the original form of $\lambda \geq 2\pi\sqrt{\chi \cdot (d\sigma/dx)^{-1}}$, obviously, Eq. (4) presents a direct explanation to the above facts, as significant stress gradient would substantially improve the incubation of shear bands and improve the plasticity of MGs.

Moreover, as predicted in **Part 3**, it is known that most MGs would prefer fracturing via a single shear band under uniaxial load, unless the primary shear band propagation is intervened in Refs. [1,2] where the subsequent deformation would be afforded by shear band multiplication. Specifically, the significant stress gradient introduced at both ends of the sample in conventional mechanical tests, especially for the constrained loading condition of compression where samples with a small aspect ratio of 2:1 compared with the samples for tensile tests are routinely used, would intervene in the propagation of shear bands largely. This would probably be the main reason why some of the MGs in Table 1 possess pronounced compressive plasticity, but rather poor tensile plasticity. If we were able to neglect the sample ends effects in the mechanical tests, the intervention of shear band propagation would be dominantly determined by the stress gradient induced by the intrinsic heterogeneous structure of MGs [1,54,55]. This is supported by the fact that MGs with pronounced free volume concentration [56] shows extraordinary plasticity by shear band multiplication. By introducing heterogeneous structure like secondary dendrite phases to intervene in the propagation of shear bands, even tensile ductility [57–59] can be designated in MG composites.

Finally, based on Eq. (4), the origin of the plastic deformation of MGs can be clearly divided as: the incubation of embryonic shear bands and the propagation of embryonic shear bands. It explains the fact that the plasticity of MGs can be pursued by increasing the shear band incubation propensity and strengthening the suppression of shear band propagation, where the stress gradients play a key role in both cases.

5. Conclusion

To summarize, an index of the shear banding susceptibility of MGs is rigorously derived as the critical strain localization factor to initiate an embryonic shear band:$\chi = \gamma_b/\gamma_m$ (γ_b shear strain in the embryonic shear band and γ_m in the matrix). The roles of the physical properties as Poisson ratio, Young's modulus and the surface energy density in the plasticity of MGs are unraveled. A potential universal correlation between the plasticity of solids and geometric compatibility is revealed.

Acknowledgments

The work is supported by the Nature Science Foundation of China (Grants Nos. 11132011, 11202221, and 11472287), the National Basic Research Program of China (Grants No. 2012CB937500), and the CAS/SAFEA International Partnership Program for Creative Research Teams.

Appendix A. Supplementary data

Supplementary data related to this article can be found at http://dx.doi.org/10.1016/j.intermet.2015.11.010.

References

[1] C.A. Schuh, T. Hufnagel, U. Ramamurty, Mechanical behavior of amorphous alloys, Acta Mater 55 (2007) 4067–4109.
[2] M.W. Chen, Mechanical behavior of metallic glasses: microscopic understanding of strength and ductility, in: Ann. Rev. Mater. Res, Ann. Rev., Palo Alto, 2008, pp. 445–469.
[3] W.H. Wang, C. Dong, C.H. Shek, Bulk metallic glasses, Mater. Sci. Eng. R Rep 44 (2004) 45–89.
[4] A.L. Greer, Y.Q. Cheng, E. Ma, Shear bands in metallic glasses, Mater. Sci. Eng. R Rep. 74 (2013) 71–132.
[5] F. Spaepen, A microscopic mechanism for steady state inhomogeneous flow in metallic glasses, Acta Metall. 25 (1977) 407–415.
[6] S.X. Song, T.G. Nieh, Direct measurements of shear band propagation in metallic glasses – an overview, Intermetallics 19 (2011) 1968–1977.
[7] Y. Shao, K.F. Yao, M. Li, X. Liu, Two-zone heterogeneous structure within shear bands of a bulk metallic glass, Appl. Phys. Lett. 103 (2013).
[8] M.W. Chen, A. Inoue, W. Zhang, T. Sakurai, Extraordinary plasticity of ductile bulk metallic glasses, Phys. Rev. Lett. 96 (2006) 245502.
[9] L.H. Dai, M. Yan, L.F. Liu, Y.L. Bai, Adiabatic shear banding instability in bulk metallic glasses, Appl. Phys. Lett. 87 (2005) 141916.
[10] M.Q. Jiang, L.H. Dai, On the origin of shear banding instability in metallic glasses, J. Mech. Phys. Solids 57 (2009) 1267–1292.
[11] L. Wang, Z.P. Lu, T.G. Nieh, Onset of yielding and shear band nucleation in an Au-based bulk metallic glass, Scr. Mater. 65 (2011) 759–762.
[12] D. Rodney, A. Tanguy, D. Vandembroucq, Modeling the mechanics of amorphous solids at different length scale and time scale, Model. Simul. Mater. Sci. Eng. 19 (2011) 083001.
[13] L.Y. Chen, B.Z. Li, X.D. Wang, F. Jiang, Y. Ren, P.K. Liaw, J.Z. Jiang, Atomic-scale mechanisms of tension–compression asymmetry in a metallic glass, Acta Mater. 61 (2013) 1843–1850.
[14] Y. Chen, M.Q. Jiang, Y.J. Wei, L.H. Dai, Failure criterion for metallic glasses, Philos. Mag. 91 (2011) 4536–4554.
[15] Y.H. Liu, G. Wang, R.J. Wang, Q. Zhao de, M.X. Pan, W.H. Wang, Super plastic bulk metallic glasses at room temperature, Science 315 (2007) 1385–1388.
[16] M.D. Demetriou, M.E. Launey, G. Garrett, J.P. Schramm, D.C. Hofmann, W.L. Johnson, R.O. Ritchie, A damage-tolerant glass, Nat. mater. 10 (2011) 123–128.
[17] F. Shimizu, S. Ogata, J. Li, Yield point of metallic glass, Acta Mater. 54 (2006) 4293–4298.
[18] A.S. Argon, Plastic deformation in metallic glasses, Acta Metall. 27 (1979) 47–58.
[19] Z. Han, W.F. Wu, Y. Li, Y.J. Wei, H.J. Gao, An instability index of shear band for plasticity in metallic glasses, Acta Mater. 57 (2009) 1367–1372.
[20] M.D. Demetriou, M. Floyd, C. Crewdson, J.P. Schramm, G. Garrett, W.L. Johnson, Liquid-like platinum-rich glasses, Scr. Mater. 65 (2011) 799–802.
[21] R.D. Conner, W.L. Johnson, N.E. Paton, W.D. Nix, Shear bands and cracking of metallic glass plates in bending, J. Appl. Phys. 94 (2003) 904–911.
[22] R.D. Conner, Y. Li, W.D. Nix, W.L. Johnson, Shear band spacing under bending of Zr-based metallic glass plates, Acta Mater. 52 (2004) 2429–2434.
[23] Y. Chen, M.Q. Jiang, L.H. Dai, Collective evolution dynamics of multiple shear bands in bulk metallic glasses, Inter. J. Plast. 50 (2013) 18–36.
[24] L.H. Dai, L.F. Liu, Y.L. Bai, Formation of adiabatic shear band in metal matrix composites, Inter. J. Solids Struct. 41 (2004) 5979–5993.
[25] W.D. Nix, H.J. Gao, Indentation size effects in crystalline materials: a law for strain gradient plasticity, J. Mech. Phys. Solids 46 (1998) 411–425.
[26] J.F. Nye, Some geometrical relations in dislocated crystals, Acta Metall. 1 (1953) 153–162.
[27] M.F. Ashby, The deformation of plastically non-homogeneous materials, Philos. Mag. 21 (1970) 399–424.
[28] A.S. Argon, M. Salama, The second international conference on rapidly quenched metals the mechanism of fracture in glassy materials capable of some inelastic deformation, Mater. Sci. Eng. 23 (1976) 219–230.
[29] W.L. Johnson, K. Samwer, A universal criterion for plastic yielding of metallic glasses with a $(T/T_g)^{2/3}$ temperature dependence, Phys. Rev. Lett. 95 (2005) 195501.

[30] Y.Q. Cheng, Z. Han, Y. Li, E. Ma, Cold versus hot shear banding in bulk metallic glass, Phys. Rev. B 80 (2009) 134115.
[31] S. Ogata, F. Shimizu, J. Li, M. Wakeda, Y. Shibutani, Atomistic simulation of shear localization in Cu-Zr bulk metallic glass, Intermetallics 14 (2006) 1033–1037.
[32] J.C. Grosskreutz, M. Mughrabi, Constitutive Equations in Plasticity, MITPress, Cambridge, MA, 1975.
[33] J. Pan, K.C. Chan, Q. Chen, L. Liu, Enhanced plasticity by introducing icosahedral medium-range order in ZrCuNiAl metallic glass, Intermetallics 24 (2012) 79–83.
[34] Y.H. Liu, W.H. Wang, Shear bands evolution in bulk metallic glass with extended plasticity, J. Non Cryst. Solids 354 (2008) 5570–5572.
[35] Q. He, Y.-Q. Cheng, E. Ma, J. Xu, Locating bulk metallic glasses with high fracture toughness: Chemical effects and composition optimization, Acta Mater. 59 (2011) 202–215.
[36] B.A. Sun, H.B. Yu, W. Jiao, H.Y. Bai, D.Q. Zhao, W.H. Wang, Plasticity of ductile metallic glasses: a self-organized critical state, Phys. Rev. Lett. 105 (2010) 035501.
[37] J. Schroers, W.L. Johnson, Ductile bulk metallic glass, Phys. Rev. Lett. 93 (2004) 255506.
[38] R. Varadarajan, A.K. Thurston, J.J. Lewandowski, Increased toughness of zirconium-based bulk metallic glasses tested under mixed mode conditions, Metall. Mater. Trans. A Phys. Metall. Mater. Sci. 41A (2010) 149–158.
[39] H. Choi-Yim, J. Schroers, W.L. Johnson, Microstructures and mechanical properties of tungsten wire/particle reinforced Zr57Nb5Al10Cu15.4Ni12.6 metallic glass matrix composites, Appl. Phys. Lett. 80 (2002) 1906–1908.
[40] C.L. Ma, A. Inoue, Microstructure and mechanical properties of Cr, Mo, Fe, Ta modified Pd-Ni-Cu-P glassy alloys prepared by copper-mold casting, Mater. Trans. 44 (2003) 188–196.
[41] B.A. Sun, W.H. Wang, The fracture of bulk metallic glasses, Prog. Mater. Sci. 74 (2015) 211–307.
[42] D.D. Liang, X.D. Wang, Y. Ma, K. Ge, Q.P. Cao, J.Z. Jiang, Decoupling of pronounced beta and alpha relaxations and related mechanical property change, J. Alloys Compd. 577 (2013) 257–260.
[43] J. Xu, U. Ramamurty, E. Ma, The fracture toughness of bulk metallic glasses, Jom 62 (2010) 10–18.
[44] Q. Jiang, H.M. Lu, M. Zhao, Modelling of surface energies of elemental crystals, J. Phys. Condes. Matter 16 (2004) 521–530.
[45] W.H. Wang, The elastic properties, elastic models and elastic perspectives of metallic glasses, Prog. Mater. Sci. 57 (2012) 487–656.
[46] G. Kumar, S. Prades-Rodel, A. Blatter, J. Schroers, Unusual brittle behavior of Pd-based bulk metallic glass, Scr. Mater. 65 (2011) 585–587.
[47] Y.F. Gao, L. Wang, H. Bei, T.G. Nieh, On the shear-band direction in metallic glasses, Acta Mater. 59 (2011) 4159–4167.
[48] A. Concustell, F.O. Mear, S. Surinach, M.D. Baro, A.L. Greer, Structural relaxation and rejuvenation in a metallic glass induced by shot-peening, Phil. Mag. Lett. 89 (2009) 831–840.
[49] Y. Wu, H.H. Wu, X.D. Hui, G.L. Chen, Z.P. Lu, Effects of drawing on the tensile fracture strength and its reliability of small-sized metallic glasses, Acta Mater. 58 (2010) 2564–2576.
[50] H. Bei, S. Xie, E.P. George, Softening caused by profuse shear banding in a bulk metallic glass, Phys. Rev. Lett. 96 (2006) 105503.
[51] Z.F. Zhang, H. Zhang, X.F. Pan, J. Das, J. Eckert, Effect of aspect ratio on the compressive deformation and fracture behaviour of Zr-based bulk metallic glass, Phil. Mag. Lett. 85 (2005) 513–521.
[52] Z.T. Wang, J. Pan, Y. Li, C.A. Schuh, Densification and strain hardening of a metallic glass under tension at room temperature, Phys. Rev. Lett. 111 (2013) 135504.
[53] W.F. Wu, Y. Li, C.A. Schuh, Strength, plasticity and brittleness of bulk metallic glasses under compression: statistical and geometric effects, Philos. Mag. 88 (2008) 71–89.
[54] K.F. Yao, F. Ruan, Y.Q. Yang, N. Chen, Superductile bulk metallic glass, Appl. Phys. Lett. 88 (2006).
[55] K.F. Yao, C.Q. Zhang, Fe-based bulk metallic glass with high plasticity, Appl. Phys. Lett. 90 (2007).
[56] L.Y. Chen, Z.D. Fu, G.Q. Zhang, X.P. Hao, Q.K. Jiang, X.D. Wang, Q.P. Cao, H. Franz, Y.G. Liu, H.S. Xie, S.L. Zhang, B.Y. Wang, Y.W. Zeng, J.Z. Jiang, New class of plastic bulk metallic glass, Phys. Rev. Lett. 100 (2008) 075501.
[57] D.C. Hofmann, J.Y. Suh, A. Wiest, G. Duan, M.L. Lind, M.D. Demetriou, W.L. Johnson, Designing metallic glass matrix composites with high toughness and tensile ductility, Nature 451 (2008) 1085–1089.
[58] Y. Wu, D.Q. Zhou, W.L. Song, H. Wang, Z.Y. Zhang, D. Ma, X.L. Wang, Z.P. Lu, Ductilizing bulk metallic glass composite by tailoring stacking fault energy, Phys. Rev. Lett. 109 (2012).
[59] Z.P. Chen, J.E. Gao, Y. Wu, H. Wang, X.J. Liu, Z.P. Lu, Designing novel bulk metallic glass composites with a high aluminum content, Sci. Rep. 3 (2013).